# Photoresponse in gate-tunable atomically thin lateral MoS$_2$ Schottky junction patterned by electron beam

Y. Katagiri, T. Nakamura, C. Ohata, S. Katsumoto, and J. Haruyama

# Photoresponse in gate-tunable atomically thin lateral MoS2 Schottky junction patterned by electron beam

Y. Katagiri,[1] T. Nakamura,[2] C. Ohata,[1] S. Katsumoto,[2] and J. Haruyama[1,2,a)]

[1]*Faculty of Science and Engineering, Aoyama Gakuin University, 5-10-1 Fuchinobe, Sagamihara, Kanagawa 252-5258, Japan*
[2]*Institute for Solid State Physics, The University of Tokyo, 5-1-5 Kashiwanoha, Kashiwa, Chiba 277-8581, Japan*

Among various atomically thin two-dimensional materials, molybdenum disulphide (MoS2) is attracting considerable attention because of its direct energy bandgap in the 2H-semiconducting phase. On the other hand, a 1T-metallic phase, which is very important for unique applications, has been created by various methods. Recently, we demonstrated the creation of in-plane 1T-metal/2H-semiconductor MoS2 lateral Schottky junctions by using electron beam irradiation techniques and revealed their unique electrical properties. Here, we report the optoelectronic measurements proving the formation of this few-layer MoS2 lateral Schottky junction. A large photocurrent is confirmed in the reverse bias voltage regime, while it decreases with increasing distance between an electrode placed on the 2H region and the 2H/1T junction. These results suggest a concentration of high electric field and rapid dissociation of photogenerated excitons at the few-layer lateral Schottky junction, which are beneficial for highly efficient photodetectors. *Published by AIP Publishing.*
[http://dx.doi.org/10.1063/1.4979831]

MoS2, one of the transition metal dichalcogenides, is currently garnering considerable interest among various atomically thin two-dimensional materials,[1,2] while its 1T-metallic phase, created by processes such as chemical doping and electron-beam (EB) and laser-beam irradiation,[3–6] is also highly valuable for some applications[3,4,7] (e.g., ohmic metallic junction between a metal electrode and 2H-MoS2[3] and supercapacitor electrodes with capacitance values up to ~700 F/cm).[3,4] An electronic transition from the 2H semiconducting MoS2 to the 1T metal phase triggered by the EB irradiation with substrate heating was observed.[5] Compared with various other synthesis methods of atom-thin MoS2 layers,[8–10] this method is highly simple and convenient because it allows formation of the 1T-metal phase MoS2 only by irradiating the EB to the 2H semiconducting phase MoS2 through the phase transition from the trigonal prismatic ($D_{3h}$) to the octahedral ($O_h$) via intralayer atomic plane gliding, which involves a transversal displacement of one of the S planes.

Based on this top-down fabrication method, we reported transport measurements indicating the formation of a lateral 2H/1T MoS2 Schottky junction with a barrier height in the range of 0.13–0.18 eV created at the interface between the EB-irradiated (1T)/non-irradiated(2H) regions.[11] The findings indicated a unique possibility of a few-layer material, of which the effective barrier height is highly sensitive to electrostatic charge doping (e.g., via back gate voltage) and is nearly free from Fermi level ($E_F$) pinning when assuming the predominance of thermionic current contribution.

On the other hand, optoelectronic properties have been reported in various atom-thin layers such as an MoS2/WS2 PN junction created by a van der Waals assembly, which exhibited a gate-tunable diode-like current rectification and a photovoltaic response across the PN interface.[12] It revealed that the tunneling-assisted interlayer recombination of the majority carriers (i.e., Shockley-Read-Hall (SRH) recombination and Langevin recombination) at the junction due to the lack of an extended depletion region is responsible for the tunability of the electronic and optoelectronic processes. The rapid separation of photogenerated charge carriers (i.e., exciton dissociation) at the PN junction was also observed through photoluminescence (PL) and photocurrent mappings. This ultrafast charge transfer was also reported in atom-thin MoS2/WS2 heterostructures.[13] However, to date, no optoelectronic properties have been observed in atom-thin 1T/2H MoS2 lateral Schottky junctions.

In the present study, 2H-phase n-type semiconducting MoS2 has been fabricated on an SiO2/Si substrate following a mechanical exfoliation method of bulk material (Smart Element Co.) using scotch tape and oxidization by exposing to air (Fig. 1(a)). Its thickness and the number of layers (approximately three layers) have been confirmed by cross sectional view of atomic force microscope, as shown in lower panel of Fig. 1(a) and also Raman spectrum. EB has been irradiated to this MoS2 with a dose of 160 Me/nm$^2$ at room temperature (Fig. 1(b)).[11] The presence of the 1T metal phase has been confirmed by X-ray photoelectron spectroscopy (XPS) and Raman spectrum, following our previous work.[11] Two electrode-pairs consisting of Ti/Au (20 nm/ 500 nm), in which one is located on the 1T-metal region (i.e., EB-irradiated region) while the other is on the 2H region, with different distance ($L_{sch}$) between the electrode formed on 2H region and 2H/1T interface have been formed on both sides of this junction for photocurrent measurements (Fig. 1(b)). Ti/Au was selected in order to obtain lower contact resistance to MoS2 layer.[14] A back-gate electrode was also

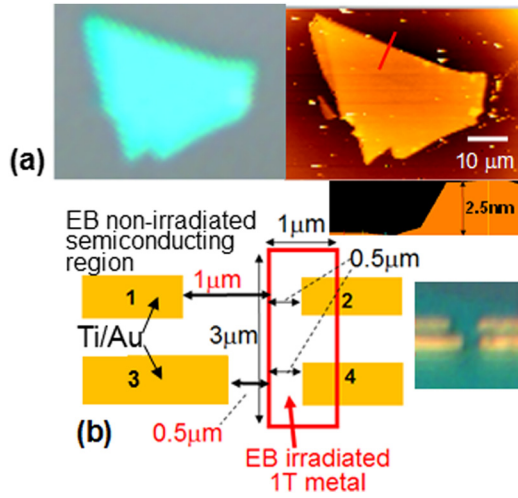a)Author to whom correspondence should be addressed. Electronic mail: J-haru@ee.aoyama.ac.jp

FIG. 1. (a) Optical (left) and atomic force (right) microscope images of top and cross-sectional views of few-layer 2H-MoS$_2$ flake fabricated by mechanical exfoliation of bulk. Cross-sectional image (right lower panel) was measured along red line noted on upper part of the flake in right main panel. (b) Schematic top view of designed two electrode-pair patterns on (a). Inset: Optical microscope image of the fabricated electrode pattern.

attached on the back-side of the Si substrate with a thick SiO$_2$ layer (~300 nm).

Figure 2(a) shows the source-drain current (I$_{sd}$) as a function of the photointensity (I$_p$) of a laser diode with a wavelength of 650 nm observed under the forward and reverse voltage bias (V$_{sd}$) regions in the lateral Schottky junction with L$_{sch}$ = 0.5 $\mu$m (see Fig. 1(b)). Through all V$_{sd}$ regions, I$_{sd}$ monotonically increases as I$_p$ increases. In

particular, the increase is significant in the reverse voltage (i.e., −V$_{sd}$) region. I$_{sd}$ vs. I$_p$ relationships for individual ±V$_{sd}$ are shown in Fig. 2(b). Drastic increases in I$_{sd}$ with increasing I$_p$ under −V$_{sd}$ are quantitatively evident.

Figures 2(c) and 2(d) are the same measurements as those in Figs. 2(a) and 2(b), respectively, but for L$_{sch}$ = 1 $\mu$m. I$_{sd}$ decrease in all voltage and I$_P$ regions, compared with those in Figs. 2(a) and 2(b). In particular, the decrease is significant in −V$_{sd}$ region. The slope values of the I$_{sd}$ vs. I$_p$ relationship for −V$_{sd}$ region drastically decreases in Fig. 2(d), compared with those in Fig. 2(b).

The back-gate voltage (V$_{bg}$) dependence of I$_{sd}$ under fixed −V$_{sd}$ regions of Fig. 2(a) is demonstrated in Fig. 3. The increase in I$_{sd}$ is significant in the +V$_{bg}$ region. Substantial increases in I$_{sd}$ for +V$_{bg}$ are much more evident in Fig. 3(b).

We qualitatively discuss the observed results. The results of Fig. 2 suggest a concentration of high electric field at the 2H/1T Schottky junction induced by an applied reverse voltage (i.e., under −V$_{sd}$) because photocurrent (i.e., exciton) generation is induced by the increasing electric field (Fig. 4(a)). Indeed, the decrease in photocurrent from Figs. 2(a) and 2(b) to 2(c) and 2(d) is consistent with an increase in L$_{sch}$ from 0.5 $\mu$m to 1 $\mu$m (Fig. 1(b)), which determines the magnitude of electric field concentration at the 2H/1T junction. Larger L$_{sch}$ for Figs. 2(c) and 2(d) suppresses the concentration of electric field at the 2H/1T Schottky junction, resulting in the decrease in photocurrent. On the other hand, photoirradiated area of 2H semiconductor between electrode and the 2H/1T junction increases with increasing L$_{sch}$. This induces photogenerated electrons and current. However, this is in contradiction to the abovementioned experimental results for the L$_{sch}$ increase. This suggests that photocurrent generation arising from electric field concentration at the 2H/1T Schottky junction is a dominant mechanism for the present structure, particularly under −V$_{sd}$.

Moreover, rapid exciton dissociation due to this high electric field also strongly contributes to the generation of a large photocurrent because electrons and holes dissociated from photogenerated excitons rapidly flow into individual electrodes. As mentioned in the introduction, rapid exciton dissociation has been reported by observing the elimination of the photoluminescence signal in an atomically thin P-WS$_2$/N-MoS$_2$ vertical junction. In the present lateral Schottky junction, this effect is significantly enhanced.
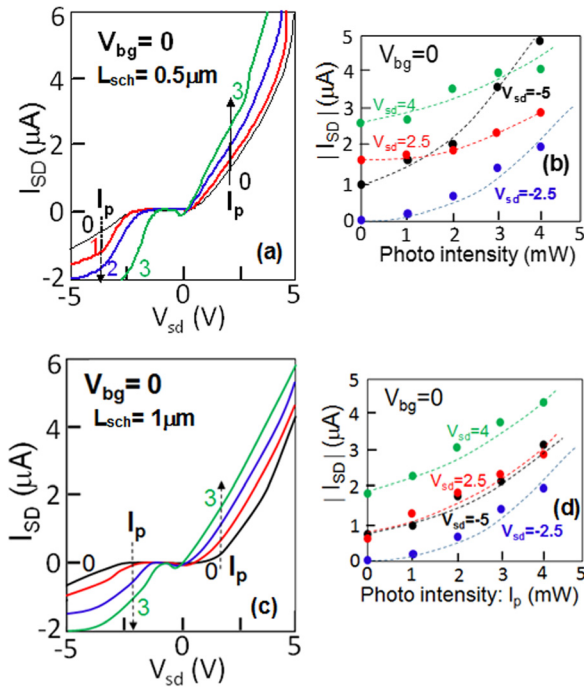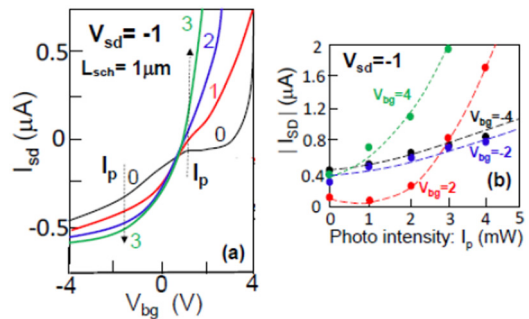


FIG. 2. (a) Source-drain current (I$_{sd}$) as a function of photointensity (I$_p$) of laser beam with the wavelength of 650 nm, observed under forward and reverse voltage bias (V$_{sd}$) regions in the lateral 2H/1T Schottky junction. Measured electrode pair corresponds to 3–4 of Fig. 1(b) with 0.5 $\mu$m of L$_{sch}$. Number noted to individual curves means I$_P$ powers in mW unit. (b) I$_{sd}$ vs. I$_p$ relationships measured at fixed individual ±V$_{sd}$ of (a). Dotted lines are included simply as a visual aid. (c) and (d) The same measurements as (a) and (b), respectively, for sample with 1$\mu$m of L$_{sch}$.



FIG. 3. (a) Back-gate voltage (V$_{bg}$) dependence of I$_{sd}$ as a function of I$_p$ under V$_{sd}$ = −1 V of Fig. 2. Number noted to individual curves means I$_P$ powers in mW unit. (b) I$_{sd}$ vs. I$_p$ relationships measured at fixed individual ±V$_{bg}$ of (a). Dotted lines are included simply as a visual aid.
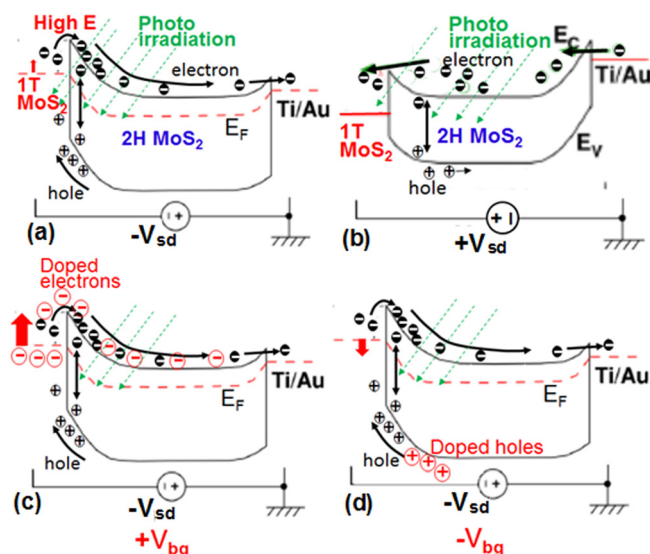
FIG. 4. Schematic views of energy band diagrams of Schottky junction for (a) reverse and (b) forward voltage regions with $V_{bg} = 0$ V, which explain the properties of Fig. 2, and for reverse voltage region under applying (c) $+V_{bg}$ and (d) $-V_{bg}$, which explain Fig. 3. For (a), high electric field concentrating at the atom-thin Schottky junction causes effective exciton generation and its rapid dissociation. For (c), applying $+V_{bg}$ causes electron doping into the 1T phase, resulting in reduction of the Schottky barrier height and induction of the exciton generation.

For this photocurrent flow, electrons in the 1T region have to overflow into the 2H region, overcoming the Schottky barrier. This has been observed through electron doping and its accumulation in the 1T region (i.e., Fermi level shift) under applied $+V_{bg}$. Here, a small number of electrons will be generated and accumulated through photo-irradiation, even in the 1T region. Because the Fermi level in this 1T region is pinning-free, as we have reported previously, even such a small amount of electron accumulation will lead to electron flow overcoming the Schottky barrier. On the other hand, under the forward voltage region ($+V_{sd}$), a photocurrent is also generated (Fig. 4(b)). However, small electric fields at the 2H/1T junction interface do not induce a photocurrent. Moreover, the contribution of photogenerated holes is less than in the case of $-V_{sd}$ because holes cannot run through the n-type $MoS_2$ into the electrode. These results support the presence of a lateral Schottky junction at the interface of the 2H/1T regions.

The results of Fig. 3 are consistent with the observation of the drastic increase in $I_{sd}$ caused by electron doping and accumulation in the 1T region by applying $+V_{bg}$ under no photoirradiation (i.e., dark current) in our previous report. Because the Schottky barrier height became 0 eV by applying only $V_{bg} = +4$ V, we revealed a drastic Fermi level shift caused by the accumulation of doped electrons in the 1T region, and thus, weak Fermi level pinning even in the presence of defects, as a unique property of the atom-thin $MoS_2$ layer. This increase in $I_{sd}$ will be significantly induced by photogenerated electrons, as shown in Fig. 4(c). On the other hand, increased hole doping by applying $-V_{bg}$ also increases $I_{sd}$ with photogenerated holes, although the contribution is smaller because it decreases the Fermi level (Fig. 4(d)).

In conclusion, we demonstrated the optoelectronic measurements proving the formation of the few-layer $MoS_2$ lateral Schottky junction. A large photocurrent was confirmed in the reverse bias voltage regime of the Schottky junction, while it decreased with increasing the distance between an electrode on the 2H region and the 2H/1T junction. These results suggested a concentration of high electric field and the rapid dissociation of photogenerated excitons at the few-atom layer lateral Schottky junction. The observed photo-response promises application to high-efficiency photosensors (detectors), as well as of atom-thin optoelectronic circuits,[15,16] which eventually results in flexible and wearable in-plane integrated circuits without using three-dimensional metal wiring. This method can also be extended to 2D transition metal oxides.[17]

[1] B. Radisavljevic, A. Radenovic, J. Brivio, V. Giacometti, and A. Kis, Nat. Nanotechnol. **6**, 147 (2011).

[2] K. F. Mak, C. Lee, J. Hone, J. Shan, and T. F. Heinz, Phys. Rev. Lett. **105**, 136805 (2010).

[3] S. Cho, S. Kim, J. H. Kim, J. Zhao, J. Soek, D. H. Keum, J. Baik, D. H. Choe, K. J. Chang, K. Suenaga, and S. W. Kim, Science **349**, 625 (2015).

[4] Y.-C. Lin, D. O. Dumcenco, Y.-S. Huang, and K. Suenaga, Nat. Nanotechnol. **9**, 391 (2014).

[5] M. Acerce, D. Voiry, and M. Chhowalla, Nat. Nanotechnol. **10**, 313 (2015).

[6] X. Chia, A. Ambrosi, D. Sedmidubský, Z. Sofer, and M. Pumera, Chem. Eur. J. **20**, 17426 (2014).

[7] A. Ambrosi, Z. Sofer, and M. Pumera, Chem. Commun. **51**, 8450 (2015).

[8] M. Chowalla, H. S. Shin, G. Eda, L-J. Li, K. P. Loh, and H. Zhang, Nat. Chem. **5**, 263 (2013).

[9] Y. Wang, E. D. Gaspera, B. J. Carey, P. Atkin, K. J. Berean, R. M. Clark, I. S. Cole, Z.-Q. Xu, Y. Zhang, Q. Bao *et al.*, Nanoscale **8**, 12258 (2016).

[10] M. Okada, T. Sawazaki, K. Watanabe, T. Taniguchi, H. Hibino, H. Shinohara, and R. Kitaura, ACS Nano **8**, 8273 (2014).

[11] Y. Katagiri, T. Nakamura, A. Ishi, C. Ohata, M. Hasegawa, S. Katsumoto, G. Iannaccone, G. Fiori, S. Roche, J. Haruyama *et al.*, Nano Lett. **16**, 3788 (2016).

[12] C.-H. Lee, G. H. Lee, A. M. V. D. Zande, W. Chen, Y. Li, M. Han, X. Cui, G. Arefe, C. Nuckolls, T. F. Heinz, and J. Guo, Nat. Nanotechnol. **9**, 676 (2014).

[13] X. Hong, J. Kim, S. F. Shi, Y. Zhang, C. Jin, Y. Sun, S. Tongay, J. Wu, Y. Zhang, and F. Wang, Nat. Nanotechnol. **9**, 682 (2014).

[14] S. Walia, S. Balendhran, Y. Wang, R. Ab Kadir, A. S. Zoolfakar, P. Atkin, J. Z. Ou, S. Sriram, K. Kalantar-Zadeh, and M. Bhaskaran, Appl. Phys. Lett. **103**, 232105 (2013).

[15] Y. An, A. Behnam, E. Pop, and A. Ural, Appl. Phys. Lett. **102**, 013110 (2013).

[16] W. Zhang, C. P. Chuu, J. K. Huang, C. H. Chen, M. L. Tsai, Y. H. Chang, C. T. Liang, Y. Z. Chen, Y. L. Chueh, J. H. He, and M. Y. Chou, Sci. Rep. **4**, 3826 (2014).

[17] K. Kalantar-Zadeh, J. Z. Ou, T. Daeneke, A. Mitchell, T. Sasaki, and M. S. Fuhrer, Appl. Mater. Today **5**, 73 (2016).